USING ACCELEROMETER SIGNALS TO
CLASSIFY PREHENSILE HAND MOVEMENTS

by

Nirav R. Sheth
A Thesis
Submitted to the
Graduate Faculty
of
George Mason University
In Partial fulfillment of
The Requirements for the Degree
of
Master of Science
Computer Science

Committee:

_____	Dr. Zoran Durić, Thesis Director
_____	Dr. Gene R. Shuman, Committee Member
_____	Dr. Lynn H. Gerber, Committee Member
_____	Dr. Sanjeev Setia, Chairman, Department of Computer Science
_____	Dr. Kenneth S. Ball, Dean, Volgenau School of Engineering
Date: _____	Spring Semester 2019 George Mason University Fairfax, VA

Using Accelerometer Signals to Classify Prehensile Hand Movements

A thesis submitted in partial fulfillment of the requirements for the degree of Master of Science at George Mason University

By

Nirav R. Sheth
Bachelor of Science
Southern Polytechnic State University, 2010

Director: Dr. Zoran Durić, Associate Professor
Department of Computer Science

Spring Semester 2019
George Mason University
Fairfax, VA

Dedication

I dedicate this thesis to my dad Ravi and my mom Malvika who taught me to always respect knowledge and value learning above all else.

Acknowledgments

Taking a research project and seeing it through completion is one of the hardest things to do in life. Towards that end, I am forever grateful to my thesis advisor Dr. Zoran Durić for patiently guiding me through completion of this thesis. I would like to thank Dr. Gene Shuman; for without his work on prehensile patterns this thesis would not exist. I would also like to thank Dr. Lynn Gerber for improving my understanding of prehensile movement and for editing this thesis. Lastly, I would like to thank the love of my life Anumeha for her continuous support and gourmet meals which kept me going this past couple of years and finish this work.

Table of Contents

List of Tables

List of Figures

Abstract

USING ACCELEROMETER SIGNALS TO CLASSIFY PREHENSILE HAND MOVEMENTS

Nirav R. Sheth

George Mason University, 2019

Thesis Director: Dr. Zoran Durić

Prehensile movement is crucial for activities of daily living (ADLs) such as grooming and self-care. In humans, the hand is the primary device utilized for prehensile movements. Recognizing the relationship between a hand's prehensile patterns and accelerometer data can be instrumental in developing assisted and enhanced functional hand devices. An accelerometer measures the linear acceleration acting on the part of the body where the sensor is placed. This thesis demonstrates the usefulness of several features, based on accelerometer data, towards recognizing prehensile movement of the hand while performing 47 movements, grips and neutral rest. Particular emphasis is given to measuring the usefulness of the features to identify movement transitions. A random forest classifier is used to recognize motion onset and offset as well as various phases of movement. The results showed that the accelerometer-based features were effective in recognizing motion onset and offset and moments of transitions. However, they were not as effective in recognizing various phases of prehensile movement.

Chapter 1: Introduction

The ability to grasp, known as prehensile movement, is important for an individual to perform basic activities of daily living (ADLs). ADLs are critical for survival and for independent living. ADLs include feeding, mobility, performing personal hygiene, administering self-care, etc. Besides walking, most ADLs are performed through upper extremity (UE) movements. In addition to ADLs, UE movements are critical for work activities and self-defense. The hand is the terminal UE device and thus utilized most for prehensile movements. Machine recognition of the hand's prehensile patterns can be instrumental in developing assisted and enhanced living devices. Such devices include robotic hands, gesture-based touch-less interfaces, assisted typing software, and more. A hand can move with multiple degrees of freedom and form different grip types due to various joints in the skeletal structure. Therefore, recognizing prehensile hand movements is challenging and requires precision.

1.1 Purpose

This thesis explores the usefulness of various Accelerometer (ACC)-based features in detecting hand movements. The random forest (RF) machine learning method is used to compare performance of ACC features in detecting motion onset and offset as well as various phases of hand movements. This thesis further explores the effectiveness of ACC features specifically around motion transition.

The first part of detecting hand movement is to recognize and differentiate between motion onset and offset. Motion onset is the moment when an object starts initial motion from neutral rest or a stationary grip position. While motion offset is when an object

returns, from motion, back to neutral rest or a stationary grip. The second part of detecting hand movement is to recognize and differentiate between various phases of movement. For example, when utilizing a hammer to insert a nail, a subject will grip the hammer, raise the hammer, lower the hammer, and return to resting position.

An accelerometer sensor is a device that measures acceleration in its own instantaneous rest frame. The ACC data utilized were collected as part of research performed by [1] that used Electromyogram (EMG) and ACC signals measured in the arm, the wrist and the hand during 47 hand movements, grips, and neutral rest. This thesis used ACC data to:

- Develop three features using the mathematics of rigid body motion and four features from raw ACC data, for a total of seven features
- Train a RF classifier for the two class problem, which detects motion onset and offset, and then for the all class problem, which tries to detect all phases of movement
- Develop a technique to measure recognition performance around motion transition

The aim of this research was to demonstrate that ACC improves classification accuracy, specifically around transitions, for prehensile hand movement. Objective one was to research seven features from ACC data and how they describe various aspects of hand movement. Objective two was to utilize these features to improve overall accuracy for classifying prehensile hand movements. Objective three was to utilize these features to improve classification accuracy around motion transition. The initial hypothesis was that ACC data at the very least can improve overall and transition classification accuracy for the two class problem. Classification accuracy is measured by the percentage of predictions, made by the classifier, that match the labels, provided by [1], for each sample in the test data.

1.2 Results Summary

The results showed that ACC-based features when combined, were effective in classifying motion onset and offset with average classification accuracy of 86.45%. The features used were also very effective in detecting transitions for both the two class and the all class problems with average transition detection time variances of 31.12 ms and 30.91 ms respectively. The feature based on the direction of axis of rotation of the gravity vector (DIR) was the most effective. It provided two class classification accuracy of approximately 82% and a transition detection time variance of approximately 36ms. However, the classification accuracy for the all class problem was a bit less 74.91%, showcasing the difficulty for machine learning techniques to differentiate between all phases of prehensile movement.

Chapter 2: Background

2.1 Muscle Movements and Grips

Hand movement is caused by contraction or relaxation of nearby muscles. Different combinations of muscle contractions and, or relaxations permit different hand movements. To cause muscle contraction or relaxation the brain sends low-level electrical, or myoelectric, signals. Electromyography (EMG) is the study of these low-level electrical, myoelectric signals [2]. EMG signals emitted from the muscles that control movement can be captured by sensors placed at key locations. EMG uses two types of sensors: needle-based, and surface-based (sEMG). sEMGs are less invasive and have been shown to provide reasonable results compared to needle-based approaches [3]. Interested readers may consult [4] Chapter 14 for more detail on "Biomechanics of the Wrist and Hand".

2.2 Accelerometers

The ACC sensor provides kinematic information based on measuring 'proper acceleration'. Proper acceleration is measured in the inertial frame of the object as compared to the earth's reference frame or some other reference frame [5]. The sensor reports the linear acceleration exerted on it, in three dimensions (x, y, and z) of its frame and in the unit of g (acceleration due to gravity at earth's surface). Therefore, at a given instant in time the sensor measures the acceleration exerted on the object by forces that cause movement. At rest position the only acceleration displayed by the sensor is the one exerted by gravity with magnitude 1g. If the sensor is at rest on a flat table the acceleration exerted by gravity will be in the negative z direction of the sensor's frame. If the sensor is at rest at an angle compared to the flat table the acceleration exerted by gravity will be split in appropriate directions of the sensor's

frame; however, the magnitude will still be 1g. When the sensor is at rest at an angle or in motion the direction of gravity will change in the sensor's inertial frame. This change in direction of gravity in the sensor's frame, can be used to calculate the pitch, roll, and yaw of the sensor from its initial position. Accelerometers are used to measure orientation and directional movement of an object. They are commonplace in todays world. They are used in navigation systems for missiles, air crafts, and drones and used for tilt sensing in tablet computers, smart phones, and digital cameras. Additionally, accelerometers are already being used in biological research to record and measure movements of both human and animal subjects.

The DelySys Trigno sensors used to record ACC data also records EMG signals. EMG signals are recorded in a very low voltage range compared to ACC signals. Researchers have shown in [6] that the correlation between EMG and ACC is low for general movement but it is strong when measuring UE movements and provide a measure of different aspects of movements in a complementary way.

2.3 Data Used

The ACC data used were collected as part of research done by [1]. The DelSys Trigno Wireless sensors were used for both EMG and ACC signals. The ACC data was collected at a rate of 148.1 Hz. Data were collected from five subjects who performed a set of 46 specific grips and movements with their hands. The data recorded involved fine motor movements and grips required to perform ADLs. The 46 grips and movements were divided into eight grip families (Hammer, Jar Lid, Ball Squeeze, Door Knob, Key, Scissors, 3-Jaw Chuck, and Tip Pinch). Each subject performed a scripted series of movements for each of the eight grip families. A series of movements consisted of the subject first maintaining their hand and arm in neutral or rest (NR) position and then performing the scripted grip and movements. At the end of the movement the subject would return to the NR position and repeat the same scripted actions again. A series consisted of total time of 2 minutes

Figure 2.1: Trigno kit used for data collection (left, top and bottom) and a subject (right) performing a jar lid turn with ten sensors attached to the action arm[1]

(120 seconds). The table 2.1 shows a description of 46 specific grips and movements with neutral rest.

Ten EMG and ACC sensors were used and placed around a subject's hand and arm. Seven of the sensors recorded EMG data only and were placed over the arm muscles that are believed to perform grips and movements, which are of interest to this research. Out of the remaining three, two sensors recorded ACC data only and were placed on the base of the thumb and on the base of the little finger. The last sensor recorded both EMG and ACC data and was placed on the extensor indicis. Table 2.2 shows sensor placements and Figure 2.1 shows the Trigno kit and a subject during the jar lid movement [1].

Table 2.1: The 47 activities (grips and associated movements) used in the analysis of the captured data[1]

No.	Grip	Code	Activity Description
1	none	NR	neutral/rest
2	hammer	HGIN	hammer grip - transition in
3	hammer	HG	hammer grip
4	hammer	HR	hammer raise
5	hammer	HGR	hammer grip - raised position
6	hammer	HL	hammer lower
7	hammer	HLOUT	hammer lower - transition out
8	jar lid	JLGIN	jar lid grip - trans.in
9	jar lid	JLG	jar lid grip
10	jar lid	JLP	jar lid turn - pronation
11	jar lid	JLRP	jar lid - rest/pause
12	jar lid	JLS	jar lid turn - supination
13	jar lid	JLOUT	jar lid - transition out
14	ball	BGIN	ball grip - transition in
15	ball	BG	ball grip
16	ball	BSQ	ball squeeze
17	ball	BSQOUT	ball squeeze - transition out
18	door knob	DKGIN	door knob grip - transition in
19	door knob	DKG	door knob grip
20	door knob	DKTS	door knob turn - supination
21	door knob	DKTR	door knob turn - rest/pause
22	door knob	DKTP	door knob turn - pronation
23	door knob	DKTOUT	door knob turn - transition out
24	key	KGIN	key grip - transition in
25	key	KG	key grip
26	key	KGTS	key turn - supination
27	key	KGTR	key grip turn - rest/pause
28	key	KGTP	key turn - pronation
29	key	KGOUT	key grip - transition out
30	scissors	SCGIN	scissors grip - transition in
31	scissors	SCG	scissors grip
32	scissors	SCO	scissors open
33	scissors	SCGO	scissors grip - open position
34	scissors	SCC	scissors close
35	scissors	SCOUT	scissors grip - transition out
36	3-jaw chuck	3JCGIN	3-jaw chuck grip - transition in
37	3-jaw chuck	3JCGIN	3-jaw chuck grip
38	3-jaw chuck	3JCR	3-jaw chuck raise
39	3-jaw chuck	3JCGR	3-jaw chuck grip - raised
40	3-jaw chuck	3JCL	3-jaw chuck lower
41	3-jaw chuck	3JCOUT	3-jaw chuck grip - transition out
42	tip pinch	TPGIN	tip pinch grip - transition in
43	tip pinch	TPG	tip pinch grip
44	tip pinch	TPR	tip pinch raise
45	tip pinch	TPGR	tip pinch grip - raised position
46	tip pinch	TPL	tip pinch lower
47	tip pinch	TPLOUT	tip pinch grip - transition out

Table 2.2: Location of the ten sensors and data collected[1]

Sensor #	Muscle location	Data collected
1	Extensor digitorum	EMG
2	Extensor indicis	EMG and ACC
3	Flexor carpi radialis	EMG
4	Flexor digitorum superficialis	EMG
5	Flexor carpi ulnaris	EMG
6	Pronator quadratus	EMG
7	Brachioradialis	EMG
8	Biceps brachii	EMG
9	Base of the thumb	ACC
10	Base of little finger	ACC

2.4 Data Processing

Real life sensor data are usually very noisy. The data must be filtered of noise to emphasize the high information sections. To filter the data, we must apply a low pass filter. A low pass filter removes high frequency components of the signal, which are typically associated with noise. We can adjust the cutoff frequency threshold by increasing or narrowing the size of the filter. If we increase the filter size, we lower the cutoff frequency thus we may eliminate a lot of noise, but we may also eliminate key informative part of the signal. Thus, we must keep the filter size small enough, so we can eliminate as much noise as possible while retaining most of the informative part of the signal.

A popular approach to filtering is to use the Gaussian filter. The Gaussian filter for one dimensional data in spatial domain takes the following form:

$$f(x) = \frac{1}{\sqrt{2\pi\sigma^2}} e^{\frac{-x^2}{2\sigma^2}} \tag{2.1}$$

Where σ represents the standard deviation of the Gaussian distribution and is parameterized to control the intensity of filtering. Filtering intensity, controlled by the size of the filter, must be balanced to ensure only the noise is reduced and not the high information sections

of the data. For sensor data, the Gaussian filter is applied by the process of convolution.

2.5 Features

Magnitude In machine learning, the magnitude of three-dimensional data is usually calculated using the L2 norm as $l2(v) = \sqrt{x^2 + y^2 + z^2}$. There are other techniques for calculating the magnitude such as the L1 norm $l1(v) =\mid x \mid + \mid y \mid + \mid z \mid$ and the Max norm as $l1(v) = max(\mid x \mid + \mid y \mid + \mid z \mid)$. However, functionally the L2 norm is the most popular and correlates best with three-dimensional data.

First Derivative The first derivative is a commonly used feature for many vision applications because it is instrumental in determining changes in pattern. Similarly, the first derivative can be useful for detecting changes in pattern in signal data from accelerometers. The first derivative of sensor data is approximated by taking differences between successive data values and dividing by differences between successive time markers. Since sampling rate is constant at 148Hz, we can simply take the difference between successive data values.

Change of Angle of the Gravity Vector The values provided by the accelerometer at an instant in time consists of the acceleration values in a three-dimensional (x, y, z) inertial frame. The acceleration values inherently take into account a constant acceleration of 1g, due to gravity, in the negative z direction of the earth's reference. Thus, two successive readings of ACC data along with vector algebra can be used to calculate the angular change in gravity vector direction. Let $\mathbf{a}$ and $\mathbf{b}$ be two successive sensor readings of ACC data. Based on vector algebra, the dot product $\mathbf{a}\cdot\mathbf{b}$ provides the angle α between the two vectors as shown in figure 2.2.

The angle α can be further calculated using the following formula:

$$\alpha = \cos^{-1} \frac{\mathbf{a} \cdot \mathbf{b}}{\mid \mathbf{a} \mid\mid \mathbf{b} \mid} \tag{2.2}$$

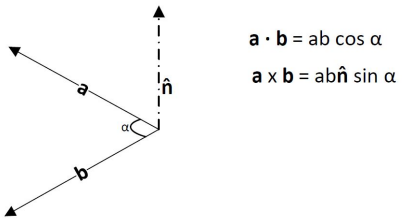

Figure 2.2: Dot and Cross Products.

Direction of Axis of Rotation of the Gravity Vector The normal vector $\hat{\mathbf{n}}$ from figure 2.2 represents the axis of rotation during motion. Thus, using two successive ACC reading one can determine the (x, y, z) components of the normal vector using the following formula:

$$\hat{\mathbf{n}} = \frac{1}{\mid \mathbf{a} \mid\mid \mathbf{b} \mid \sin\alpha} \mathbf{a} \times \mathbf{b} \tag{2.3}$$

Pitch and Roll Accelerometer readings capture forces acting on the sensor. These forces consist of gravity and the linear acceleration in x, y, and z directions of the sensor's inertial coordinate frame. Assume that a sensor's inertial coordinate frame at time t_0 is such that the gravity acts in the negative z direction; indicated by figure 2.3(a). Then at time t_1 the sensor's frame changes due to motion; figure 2.3(c). The rotational change in a sensor's coordinate frame can be captured by rotation about all three x, y, and z axes. The rotation about x axis is called roll $\mathbf{R}_x(\phi)$, y axis is called pitch $\mathbf{R}_y(\theta)$, and z axis is called yaw $\mathbf{R}_y(\psi)$ figure 2.3(b). The mathematical relation between two ACC readings for rigid body rotation is expressed using the following formula: $\mathbf{a}_1 = \mathbf{R}_{01} \cdot \mathbf{a}_0$; where the rotation matrix $\mathbf{R}_{01} = \{\mathbf{R}_x(\phi)\ \mathbf{R}_y(\theta)\ \mathbf{R}_y(\psi)\}$[7]. Using Euler angles we can represent the Pitch, Roll, and Yaw as:

$$\mathbf{R}_x(\phi) = \begin{bmatrix} 1 & 0 & 0 \\ 0 & \cos\phi & -\sin\phi \\ 0 & \sin\phi & \cos\phi \end{bmatrix} \tag{2.4}$$

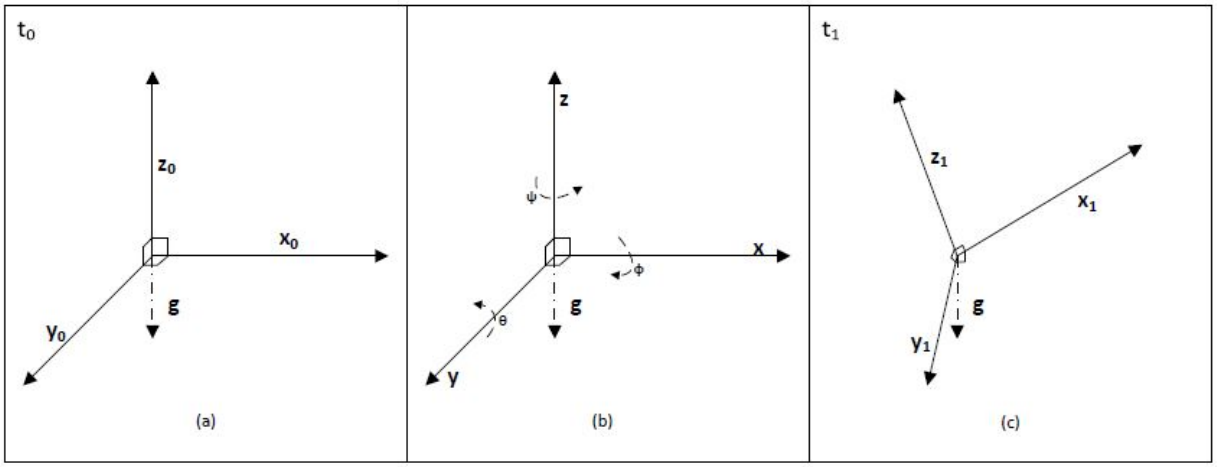

Figure 2.3: Pitch θ, Roll ϕ, and Yaw ψ. (a) Sensor frame at t_0. (b) Rotation about x, y, and z. (c) Sensor frame at t_1

$$\mathbf{R}_y(\theta) = \begin{bmatrix} \cos\theta & 0 & \sin\theta \\ 0 & 1 & 0 \\ -\sin\theta & 0 & \cos\theta \end{bmatrix} \tag{2.5}$$

$$\mathbf{R}_z(\psi) = \begin{bmatrix} \cos\psi & -\sin\psi & 0 \\ \sin\psi & \cos\psi & 0 \\ 0 & 0 & 1 \end{bmatrix} \tag{2.6}$$

There are six different orders in which the sensor frame can be rotated $\{\mathbf{R}_{xyz}, \mathbf{R}_{xzy}, \mathbf{R}_{yzx}, \mathbf{R}_{yxz}, \mathbf{R}_{zxy}, \mathbf{R}_{zyx}\}$. For the purposes of this thesis the order of rotation doesn't matter since we are looking for features that measure relative differences. Thus we decide to use $\mathbf{R}_{xyz}$ which is widely used in the aerospace industry and is known as the 'aerospace rotation sequence' [8]. We can also assume, irrespective of the sensor's initial position, that at some t_0 the sensor is at rest on a flat table. Thus the linear acceleration is $a_0 = \begin{pmatrix} 0 & 0 & -1 \end{pmatrix}$

due to gravity. Thus $\mathbf{a}_1 = \mathbf{R}_{01} \cdot \mathbf{a}_0$ becomes $\mathbf{a}_1 = (\mathbf{R}_x(\phi)\mathbf{R}_y(\theta)\mathbf{R}_y(\psi)) \begin{pmatrix} 0 \\ 0 \\ -1 \end{pmatrix}$. Which after substitution of Euler angles and expansion result in:

$$\mathbf{a}_1 = \begin{bmatrix} -\sin\theta \\ \cos\theta\sin\phi \\ \cos\theta\cos\phi \end{bmatrix} \tag{2.7}$$

If we further normalize $\mathbf{a}_1$ to unit vectors of the coordinate frame we get:

$$\frac{\mathbf{a}_1}{\mid \mathbf{a}_1 \mid} = \frac{1}{\sqrt{x_1^2 + y_1^2 + z_1^2}} \begin{bmatrix} x_1^2 \\ y_1^2 \\ z_1^2 \end{bmatrix} = \begin{bmatrix} -\sin\theta \\ \cos\theta\sin\phi \\ \cos\theta\cos\phi \end{bmatrix} \tag{2.8}$$

Solving the above equations for roll ϕ_{xyz} and pitch $theta_{xyz}$ angles we get[8]:

$$\tan\phi_{xyz} = \frac{y_1}{z_1} \tag{2.9}$$

$$\tan\theta_{xyz} = \frac{-x_1}{\sqrt{y_1^2 + z_1^2}} \tag{2.10}$$

2.6 Classification

Machine learning algorithms enable computers to learn from existing data and improve their performance, predictions against future data. Supervised learning is a type of learning where:

"Given a **training set** of N example input-output pairs

$$(x_1, y_1), (x_2, y_2), ...(x_N, y_N),$$

where each y_j was generated by an unknown function $y = f(x)$,

discover a function h that approximates the true function f"[9].

Thus, supervised learning is also known as 'learning from example' where the hypothesis function h is discovered by training on example data (the training set). Classification is the case where the output y is a set of finite values such as (Yes, No, Maybe) as compared to regression where the output y is a number (e.g., speed of a car). In the context of this paper classification will be used to train the computer on ACC data where the output are labels which specify the various phases of movement, (HGIN, HGOUT, etc), grip (HG, HL, etc), or neutral rest (NR), occurring during the time period.

Decision Tree and Random Forest Decision Tree is a form of supervised learning where a given set of input features are separated at each tree node. The output values are separated at each node based on a test performed on one of the input attributes. Decision Trees is one of the simplest forms of machine learning and where the algorithm is prone to overfitting. Overfitting results in an algorithm that provides accurate predictions on learned data only. In contrast, it is not able to generalize well enough to make good predictions on any new, not previously seen, input data. However, Decision Trees are simple to implement and can make fast classification decisions.

Random Forest is a type of algorithm where multiple decision trees are randomly generated for one set of training data. The results of the different trees are then aggregated using a majority voting scheme. Random Forest improves the accuracy of decision trees and is the algorithm used in this paper to compare the effectiveness of various ACC features.

Cross-Validation Cross-Validation is an effective way to tackle the problem of overfitting and improve the generalization of machine learning algorithms. In Cross-Validation training data are split into two or more sets where one of the sets is used as test data and the rest

of the sets are used for training. The algorithm then rotates to use another set as test data and the rest as training data. This process is repeated multiple times until each set of data is used for testing. The results of the tests are then averaged to serve as the way to score the learned model.

Chapter 3: Related Work

Currently it is not possible to measure a person's intent for movement. EMG signals detect the changes in electric potential of muscles [10] and can be used to analyze human movement. However, for robotic control or assisted device applications, the intention for movement must be predicted. To that end, much research has been done using EMG-based features to anticipate movement for prosthesis control-based applications. Research done in [11] used seven different EMG-based features (Mean Absolute Value, marginal Discrete Wavelet Transform, Histogram, Waveform Length, Short-Time Fourier Transform, Variance, and Cepstral Coefficients) along with four different classifiers (Linear Discriminant Analysis, k-Nearest Neighbors, Neural Network, and Support Vector Machine (SVM)). Their research classified 52 different hand movements obtained from 27 subjects. The results showed none of the features or classifiers used exceeded 80% accuracy. The best result came from a SVM classifier trained with mean absolute value as a feature. The research also found that classification accuracy decreased during periods of movement transition.

In [12] researchers explored the possibility of going featureless. They compared an EMG control scheme with a regression convolutional neural network (CNN) to conventional regression models learned by SVM using purpose built EMG features. The results showed that CNN-based system outperformed the SVM-based system. The research showed that it is possible to extract underlying motor control information from EMG signals without developing features.

Recent research has shown that offline classification accuracy does not correlate well with real life control of prosthesis. Research done by [13] showed that an EMG-based model trained in an academic setting performed poorly in a real life setting. Their research showed

that the cause of the decrease in performance stems from the difference in distribution of EMG data between both settings.

Often EMG, being low-level electrical, signals are not strong enough to detect changes in patterns and dispersed among a group of muscles. Therefore, many research projects have started using and have shown that ACC data in combination with EMG is a good indicator of movement. In [6] research showed that there is high correlation between EMG and ACC data when trying to recognize ADLs. The research used Pearson correlation coefficients to compare ACC and sEMG data from six male subjects performing standardized tasks as well as activities of daily life (ADL). The results showed low correlations between ACC and EMG on standardized tasks but considerably higher correlations for ADL.

Research in [14] used kernelized SVM-based classification approach to compare ACC to EMG data. Their research classified 40 hand and wrist movements from 20 subjects using the NINAPRO data set. Their approach used Mean Absolute Value of a sliding time window for ACC and Root Mean Square (RMS), marginal Discrete Wavelet Transform (mDWT), and histogram for EMG. Their results showed that ACC data provided a classification accuracy of 81.33% which was significant improvement over sEMG data which provided the best classification accuracy of 78.07% with mDWT as feature. However, when both ACC and sEMG features where combined the classification accuracy moved up to 82.59%.

In [1], Shuman, et al. used several machine learning techniques on EMG data in order to classify over 47 hand movements and grips (including neutral rest). ACC data were used in order to label various phases of movements by first aligning EMG and ACC data at 500 HZ sampling rate and then visually inspecting changes in ACC signal patterns and assigning motion labels to those patterns. The results from machine learning techniques showed an accuracy of up to 75.09% in classifying 47 different grips and movements using Hidden Markov Model (HMM)s and transition matrix composed of estimating grip to grip (including rest) transition probabilities. However, when not including neutral rest transition

movements, such as from grip to rest and vice versa, the accuracy increases to about 85.68%.

For prehensile movement recognition there has been limited work done using ACC only. ACC data have been widely used to compute tilt, pitch and roll of sensors, smart phones, and other devices [8]. Researchers in [15] used ACC data to measure gait of 25 participants during a 2 min continuous walk. Their results showed good feasibility for measuring step count but varying levels of feasibility while measuring different gait characteristics.

The research reported in this paper differs from previous efforts in that it develops ACC-based features from gravity and linear accelerations. It uses the direction of gravity at rest to compute the rotational motion of the sensors. The features used are developed from change of angle of the gravity vector, the direction of rotation, and pitch and roll measurements with the XYZ rotation order. The research further compares the effectiveness of these features for classifying prehensile patterns as well as moments of transition.

Chapter 4: Technical Approach

4.1 Feature Creation

Objective one of this thesis was to develop various features based on ACC data and evaluate their effectiveness for recognizing prehensile movement. Table 4.1 shows seven features and the combined feature used in this thesis. The raw ACC data from three sensors (2, 9, and 10 from table 2.2 referred here as s_2, s_9, s_{10}) were used. Each of the three sensors recorded acceleration in x, y, and z directions, of the sensor's frame, while each of the four subjects performed movements. Each subject performed one series (120 seconds) of continuous movement run per grip family (Hammer, Jar Lid, Ball Squeeze, Door Knob, Key, Scissors, 3-Jaw Chuck, and Tip Pinch). A series of 120 second continuous movement consisted of 12 repetitions of 10 second segments. Before the raw data were used for feature creation they were filtered using a Gaussian filter with $\sigma = 2$. A Gaussian filter with $\sigma = 2$ uses a convolution filter of size 11 samples. One series of runs per grip family consisted of 120 seconds at 148 Hz sampling rate; which results in 17760 total samples per series. Therefore a convolution filter of size 11 samples is small enough so as to not remove useful information from the data.

Magnitude and Magnitude 1D The magnitude (MAG) feature consisted of the L2 norms of all three sensors. It can be represented as:

$$MAG = [\sqrt{s_{2x}^2 + s_{2y}^2 + s_{2z}^2}, \sqrt{s_{9x}^2 + s_{9y}^2 + s_{9z}^2}, \sqrt{s_{10x}^2 + s_{10y}^2 + s_{10z}^2}] \tag{4.1}$$

Table 4.1: List of features

Feature	Description
MAG	Raw magnitude from ACC data
XYZ	Raw ACC directional data in X, Y, and Z directions
MAG 1D	First Derivative of magnitude from ACC data
XYZ 1D	First Derivative of ACC directional data
CANG	Change of Angle of the Gravity Vector
DIR	Direction of the Axis of Rotation of the Gravity Vector
PR	Pitch and Roll of the ACC sensors
COMB	Combined all seven features above

The derivative (MAG 1D) consisted of the first derivatives of the L2 norms of all three sensors. It can be represented as:

$$MAG1D = [\frac{\partial\sqrt{s_{2x}^2 + s_{2y}^2 + s_{2z}^2}}{\partial t}, \frac{\partial\sqrt{s_{9x}^2 + s_{9y}^2 + s_{9z}^2}}{\partial t}, \frac{\partial\sqrt{s_{10x}^2 + s_{10y}^2 + s_{10z}^2}}{\partial t}] \tag{4.2}$$

XYZ and XYZ 1D The directional (XYZ) feature consisted of raw data in x, y, and z directions from all three sensors. It can be represented as:

$$XYZ = [s_{2x}, s_{2y}, s_{2z}, s_{9x}, s_{9y}, s_{9z}, s_{10x}, s_{10y}, s_{10z}] \tag{4.3}$$

The derivative (XYZ 1D) consisted of the first derivative of the raw data in x, y, and z directions of all three sensors. It can be represented as:

$$XYZ1D = [\frac{\partial s_{2x}}{\partial t}, \frac{\partial s_{2y}}{\partial t}, \frac{\partial s_{2z}}{\partial t}, \frac{\partial s_{9x}}{\partial t}, \frac{\partial s_{9y}}{\partial t}, \frac{\partial s_{9z}}{\partial t}, \frac{\partial s_{10x}}{\partial t}, \frac{\partial s_{10y}}{\partial t}, \frac{\partial s_{10z}}{\partial t}] \tag{4.4}$$

Change of Angle of the Gravity Vector The change of angle of the gravity vector (CANG) feature is based on the α angle value, described in equation 2.2, from all three sensors. It can be represented as:

$$CANG = [\alpha_{s2}, \alpha_{s9}, \alpha_{s10}] \tag{4.5}$$

Direction of the Axis of Rotation of the Gravity Vector The direction of the axis of rotation of the gravity Vector (DIR) feature is based on the x, y, and z components of the $\hat{\mathbf{n}}$ vector, described in equation 2.3. It can be represented as:

$$DIR = [\hat{\mathbf{n}}_{s2x}, \hat{\mathbf{n}}_{s2y}, \hat{\mathbf{n}}_{s2z}, \hat{\mathbf{n}}_{s9x}, \hat{\mathbf{n}}_{s9y}, \hat{\mathbf{n}}_{s9z}, \hat{\mathbf{n}}_{s10x}, \hat{\mathbf{n}}_{s10y}, \hat{\mathbf{n}}_{s10z}] \tag{4.6}$$

Pitch and Roll The pitch and roll (PR) feature is based on the θ and ϕ values, described in equation 2.9 and 2.10, from all three sensors. It can be represented as:

$$PR = [\theta_{s2}, \theta_{s9}, \theta_{s10}, \phi_{s2}, \phi_{s9}, \phi_{s10}] \tag{4.7}$$

Combined The combined (COMB) feature is based on the combination of all seven features above. It can be represented as:

$$COMB = [MAG, XYZ, MAG1D, XYZ1D, CANG, DIR, PR] \tag{4.8}$$

4.2 Random Forest

Random Forest is the sole classifier used to compare the various features computed from ACC data. Random Forest classifiers with up to 50 estimators were tried on data from one subject. However, due to diminishing returns in run time and no significant gain in overall accuracy from more estimators, 25 were used for final result generation. The maximum depth of trees was selected to be 10 for similar reasons of diminishing returns. Each subject's 120 seconds series run was split into 12 ten second segments. k-Fold cross-validation, with $k = 12$, was used to perform test and train splits. So there was a total of 12 runs of the classifier were each time a different 10 second segment was used for testing. The results of all 12 runs were then averaged to provide the final results for each feature per subject per grip family.

Overall accuracy was measured by the percentage of correct predictions by the classifier against the test data. Accuracy around the moments of transition was measured by the time difference between the time transition occurred in labeled movement and the time when the classifier predicted that transition occurred. Since the classifier can detect the transition before or after the actual transition time the absolute value of the time difference was used. The transition time difference is capped off at 1 second. So, if the algorithm cannot predict that a transition occurred either 148 samples before or after the actual transition time then it will return 1 second. To provide the final measure, the time differences at all moments of transition in a series were averaged. To rate the performance of a feature in detecting transitions as high we want the average time difference of a series to be less than 150 milliseconds (ms). Which is half of the 300 ms response delay which has been frequently cited as an acceptable threshold for control-based applications [16].

4.3 Experiments

The first sets of experiments were run on the two class problem where the aim of the RF classifier was to detect motion onset and offset only. In order to do this the labels for movements where altered to align with motion onset and offset. NR or Neutral Rest as well as all the labels which represented a grip were set to '0', since during these phases no motion occurred. All other labels were set to '1', representing movement. Table 4.2 details the label conversion for all family of movements.

The second sets of experiments were on the all class problem where the aim of the RF classifier was to detect all phases of motion. The default unaltered labels were used for these experiments because they represent all 47 classes of movements from rest, movement, and grips.

Table 4.2: Label Conversions for Two Class Problem

Activity Description	**Label**	**Converted Label**
neutral/rest	NR	0
hammer grip - transition in	HGIN	1
hammer grip	HG	0
hammer raise	HR	1
hammer grip - raised position	HGR	0
hammer lower	HL	1
hammer lower - transition out	HLOUT	1
jar lid grip - trans.in	JLGIN	1
jar lid grip	JLG	0
jar lid turn - pronation	JLP	1
jar lid - rest/pause	JLRP	0
jar lid turn - supination	JLS	1
jar lid - transition out	JLOUT	1
ball grip - transition in	BGIN	1
ball grip	BG	0
ball squeeze	BSQ	1
ball squeeze - transition out	BSQOUT	1
door knob grip - transition in	DKGIN	1
door knob grip	DKG	0
door knob turn - supination	DKTS	1
door knob turn - rest/pause	DKTR	0
door knob turn - pronation	DKTP	1
door knob turn - transition out	DKTOUT	0
key grip - transition in	KGIN	1
key grip	KG	0
key turn - supination	KGTS	1
key grip turn - rest/pause	KGTR	0
key turn - pronation	KGTP	1
key grip - transition out	KGOUT	1
scissors grip - transition in	SCGIN	1
scissors grip	SCG	0
scissors open	SCO	1
scissors grip - open position	SCGO	0
scissors close	SCC	1
scissors grip - transition out	SCOUT	1
3-jaw chuck grip - transition in	3JCGIN	1
3-jaw chuck grip	3JCG	0
3-jaw chuck raise	3JCR	1
3-jaw chuck grip - raised	3JCGR	0
3-jaw chuck lower	3JCL	1
3-jaw chuck grip - transition out	3JCOUT	1
tip pinch grip - transition in	TPGIN	1
tip pinch grip	TPG	0
tip pinch raise	TPR	1
tip pinch grip - raised position	TPGR	0
tip pinch lower	TPL	1
tip pinch grip - transition out	TPLOUT	1

4.4 Software APIs used

All of the software was written in Python and executed using Python 3.6. For machine learning tasks Scikit-learn library was used, specifically its RandomForestClassifier API. For general data processing Numpy and Scipy were heavily utilized. The results were generated to .CSV files and plots were generated using Matplotlib library.

Chapter 5: Results

This chapter presents the results for the four subjects and two experiments. For experiment one 47 grips and movements listed in Table 2.1 were converted to two classes as specified in Table 2.1. For experiment 2 all 47 grips and movements were used for classification. The results are analyzed and discussed in the following chapter. The results provided in section 5.1 and section 5.2 consist an average over all 8 grip families for each subject. Detailed results for each subject and each grip family are provided in section 5.3.

5.1 Experiment 1 - Two Class Problem

The two class problem consists of recognizing motion onset and offset. The stationary grips and neutral rest are classified as motion off and grip movements are considered as motion on. Table 5.1 provides overall classification accuracy for the two class problem for each subject. The overall accuracy provided in Table 5.1 are averaged over all 8 grip families. Table 5.2 provides the results of variance between predicted transition time and labeled transition time.

5.2 Experiment 2 - All Class Problem

The all class problem consists of recognizing all phases of motion individually. All 47 grips and movements were used for classification. Table 5.3 provides overall classification accuracy for the all class problem for each subject. The overall accuracy provided in Table 5.3 is averaged over all 8 grip families. Table 5.4 provides the results of variance between predicted transition time and labeled transition time.

Table 5.1: Overall classification accuracy (%) for Two Class problem

Feature	**Subject 1**	**Subject 2**	**Subject 3**	**Subject 4**
MAG	82.29	76.37	76.47	83.56
XYZ	82.19	73.3	78.69	81.49
MAG 1D	82.5	77.19	77.05	81.66
XYZ 1D	85.01	80.47	80.43	84.62
CANG	84.31	80.58	79	83.91
DIR	84.36	80.23	79.14	84.78
PR	77.19	65.48	76.08	73.64
COMB	89.03	81.78	84.09	90.89

Table 5.2: Transition detection time variance (ms) for Two Class problem

Feature	**Subject 1**	**Subject 2**	**Subject 3**	**Subject 4**
MAG	73	60	55	38
XYZ	55	57	42	36
MAG 1D	54	152	139	36
XYZ 1D	36	63	105	27
CANG	61	76	68	44
DIR	44	51	28	25
PR	63	67	46	50
COMB	32	37	31	23

Table 5.3: Overall classification accuracy (%) for ALL Class problem

Feature	**Subject 1**	**Subject 2**	**Subject 3**	**Subject 4**
MAG	61.53	52.5	56.61	69.43
XYZ	70.38	56.37	65.9	72.51
MAG 1D	45.4	36.51	39.06	45.06
XYZ 1D	55.68	46.24	49.83	55.11
CANG	49.55	41.86	45.28	49.33
DIR	58.91	48.1	52.75	61.4
PR	64.59	50.63	62.98	66.57
COMB	78.67	66.03	72.14	82.84

Table 5.4: Transition detection time variance (ms) for ALL Class problem

Feature	Subject 1	Subject 2	Subject 3	Subject 4
MAG	56	58	43	39
XYZ	41	55	38	35
MAG 1D	74	72	42	33
XYZ 1D	37	51	29	25
CANG	60	64	62	47
DIR	38	45	28	26
PR	48	64	45	47
COMB	29	41	32	23

Table 5.5: Subject 1 - Overall Accuracy(%) - Two Class

Feature	Hammer	3 Jaw Chuck	Ball Squeeze	Door Knob	Key	Scissors	Tip Pinch	Jar Lid
MAG	91.80	78.82	84.50	85.67	87.76	69.51	80.62	79.64
XYZ	87.95	77.09	80.44	86.51	84.78	75.39	82.53	82.80
MAG 1D	92.15	73.50	88.46	82.65	91.69	73.72	68.78	89.05
XYZ 1D	93.87	78.71	92.04	85.93	92.66	74.98	70.45	91.46
CANG	92.13	73.36	93.08	83.69	91.35	77.11	71.74	92.05
DIR	91.59	77.44	92.02	83.27	92.05	73.73	73.23	91.55
PR	79.50	75.91	76.20	81.23	77.12	72.58	79.50	75.47
COMB	92.93	80.69	89.59	91.70	93.58	82.69	87.59	93.45

5.3 Detailed Results

The detailed results provide insight into overall classification accuracy and transition detection time variance for each subject and each of the 8 grip families. The two class problem involves detecting motion onset and offset. The all class problem involves detecting all 47 grips, movements and neutral rest phases of motion.

Table 5.6: Subject 2 - Overall Accuracy(%) - Two Class

Feature	Hammer	3 Jaw Chuck	Ball Squeeze	Door Knob	Key	Scissors	Tip Pinch	Jar Lid
MAG	87.76	66.11	65.29	83.06	76.63	62.93	89.47	79.67
XYZ	82.07	59.66	68.52	80.79	74.52	56.80	90.56	73.47
MAG 1D	87.82	66.89	66.14	85.55	76.79	72.67	82.64	79.01
XYZ 1D	91.42	70.13	69.78	86.35	83.14	74.75	83.57	84.60
CANG	89.77	67.91	72.66	86.58	82.15	76.27	85.21	84.09
DIR	89.63	68.70	70.55	85.82	82.32	75.74	85.04	84.04
PR	64.33	53.04	66.74	70.91	69.90	50.19	87.70	61.05
COMB	89.96	66.52	73.59	87.88	85.95	74.73	91.37	84.23

Table 5.7: Subject 3 - Overall Accuracy(%) - Two Class

Feature	Hammer	3 Jaw Chuck	Ball Squeeze	Door Knob	Key	Scissors	Tip Pinch	Jar Lid
MAG	86.61	75.11	75.85	70.27	78.19	67.78	81.00	76.98
XYZ	84.85	75.67	81.11	77.87	70.01	76.59	81.43	81.99
MAG 1D	83.58	70.94	82.98	74.11	78.82	73.29	76.15	76.53
XYZ 1D	87.35	76.73	87.37	76.59	83.21	75.75	76.14	80.28
CANG	84.13	68.29	88.90	74.06	82.47	78.04	75.75	80.33
DIR	85.25	74.21	85.34	74.28	82.19	74.76	77.67	79.41
PR	84.21	69.26	77.46	75.67	68.15	74.59	81.58	77.75
COMB	90.73	80.16	88.94	79.83	83.21	82.35	80.97	86.49

Table 5.8: Subject 4 - Overall Accuracy(%) - Two Class

Feature	Hammer	3 Jaw Chuck	Ball Squeeze	Door Knob	Key	Scissors	Tip Pinch	Jar Lid
MAG	91.29	85.21	76.04	83.42	80.01	79.29	90.58	82.60
XYZ	87.76	83.45	72.08	86.73	70.27	79.68	92.77	79.15
MAG 1D	90.21	88.64	77.73	71.94	85.75	81.44	73.83	83.75
XYZ 1D	92.75	91.37	81.50	76.46	87.59	84.10	78.80	84.36
CANG	91.13	89.35	85.82	73.03	85.78	85.04	77.69	83.47
DIR	90.61	90.48	79.66	76.40	87.30	85.04	86.29	82.50
PR	75.02	72.77	63.39	81.38	62.65	78.87	87.18	67.85
COMB	94.41	92.58	90.00	91.87	89.22	88.04	95.17	85.86

Table 5.9: Subject 1 - Transition time variance(ms) - Two Class

Feature	Hammer	3 Jaw Chuck	Ball Squeeze	Door Knob	Key	Scissors	Tip Pinch	Jar Lid
MAG	29	279	37	46	50	60	43	38
XYZ	35	84	51	35	85	41	59	52
MAG 1D	24	193	34	49	32	32	39	25
XYZ 1D	16	133	23	20	23	26	19	27
CANG	29	211	31	42	34	60	52	32
DIR	17	157	37	28	27	25	21	35
PR	36	84	78	51	95	38	61	60
COMB	14	89	29	27	19	28	29	25

Table 5.10: Subject 2 - Transition time variance(ms) - Two Class

Feature	Hammer	3 Jaw Chuck	Ball Squeeze	Door Knob	Key	Scissors	Tip Pinch	Jar Lid
MAG	40	156	61	50	38	40	26	68
XYZ	30	107	64	54	52	65	34	48
MAG 1D	25	156	46	35	24	29	873	26
XYZ 1D	16	185	59	28	21	24	147	23
CANG	29	183	147	34	34	43	101	38
DIR	21	178	59	30	26	27	39	30
PR	53	70	76	78	68	68	49	71
COMB	17	106	48	24	22	36	21	27

Table 5.11: Subject 3 - Transition time variance(ms) - Two Class

Feature	Hammer	3 Jaw Chuck	Ball Squeeze	Door Knob	Key	Scissors	Tip Pinch	Jar Lid
MAG	47	64	43	37	37	33	147	32
XYZ	38	52	51	41	40	39	46	30
MAG 1D	32	41	47	46	28	27	858	33
XYZ 1D	28	33	35	35	25	26	632	29
CANG	49	50	70	49	63	38	142	83
DIR	21	30	31	22	23	22	49	24
PR	42	65	51	37	49	39	49	38
COMB	27	33	36	28	31	25	43	27

Table 5.12: Subject 4 - Transition time variance(ms) - Two Class

Feature	Hammer	3 Jaw Chuck	Ball Squeeze	Door Knob	Key	Scissors	Tip Pinch	Jar Lid
MAG	31	38	38	32	56	52	21	38
XYZ	32	31	41	24	52	41	32	37
MAG 1D	28	28	27	45	24	28	73	40
XYZ 1D	21	25	21	19	21	24	52	34
CANG	35	54	42	30	35	33	75	51
DIR	23	29	27	18	23	28	18	36
PR	43	46	49	45	64	39	65	46
COMB	19	29	24	20	23	21	23	28

Table 5.13: Subject 1 - Overall Accuracy(%) - All Class

Feature	Hammer	3 Jaw Chuck	Ball Squeeze	Door Knob	Key	Scissors	Tip Pinch	Jar Lid
MAG	57.48	65.79	62.84	61.57	70.28	43.36	67.85	63.05
XYZ	77.79	67.62	71.08	68.36	77.55	63.80	69.41	67.42
MAG 1D	50.20	37.74	64.82	45.51	49.34	30.78	41.91	42.93
XYZ 1D	63.93	49.33	71.39	58.50	56.78	39.75	53.57	52.21
CANG	53.55	36.90	65.41	48.07	54.10	37.92	47.61	52.86
DIR	73.30	59.69	65.32	56.77	62.55	43.88	57.37	52.41
PR	71.17	66.51	68.13	61.28	68.67	59.86	59.23	61.83
COMB	86.93	72.11	80.93	73.19	87.62	71.12	82.58	74.89

Table 5.14: Subject 2 - Overall Accuracy(%) - All Class

Feature	Hammer	3 Jaw Chuck	Ball Squeeze	Door Knob	Key	Scissors	Tip Pinch	Jar Lid
MAG	70.69	46.75	47.45	55.86	58.47	27.03	65.69	48.05
XYZ	74.92	44.64	58.21	57.69	61.84	30.66	75.33	47.68
MAG 1D	41.42	30.76	44.65	39.37	38.59	29.85	33.04	34.43
XYZ 1D	57.85	39.97	49.31	46.30	50.50	34.22	49.59	42.15
CANG	49.65	33.35	50.28	43.87	41.38	34.23	40.51	41.61
DIR	57.62	46.17	47.79	45.60	53.32	33.63	59.21	41.43
PR	62.39	43.19	58.28	47.96	52.31	28.97	69.62	42.34
COMB	86.67	56.41	64.28	65.66	73.62	41.51	80.24	59.84

Table 5.15: Subject 3 - Overall Accuracy(%) - All Class

Feature	Hammer	3 Jaw Chuck	Ball Squeeze	Door Knob	Key	Scissors	Tip Pinch	Jar Lid
MAG	67.92	55.92	66.39	49.52	62.81	43.59	51.28	55.42
XYZ	77.33	60.16	78.92	60.38	62.65	67.68	51.95	68.14
MAG 1D	51.40	33.42	56.88	32.98	41.80	28.38	29.77	37.87
XYZ 1D	62.73	49.78	65.25	42.06	49.90	35.89	43.73	49.29
CANG	56.54	38.09	65.77	36.15	46.09	34.87	36.87	47.86
DIR	60.09	53.29	62.51	47.24	55.12	40.48	51.90	51.37
PR	74.62	56.78	75.58	57.29	60.92	64.75	47.02	66.91
COMB	83.39	69.38	84.88	62.80	71.26	71.51	62.11	71.78

Table 5.16: Subject 4 - Overall Accuracy(%) - All Class

Feature	Hammer	3 Jaw Chuck	Ball Squeeze	Door Knob	Key	Scissors	Tip Pinch	Jar Lid
MAG	79.21	75.32	62.88	70.50	69.65	62.49	73.49	61.87
XYZ	81.00	77.22	69.17	70.31	66.11	71.34	76.77	68.19
MAG 1D	44.59	50.46	45.42	45.97	40.69	38.18	46.10	49.07
XYZ 1D	59.46	62.21	55.51	56.45	49.22	45.65	56.57	55.84
CANG	56.73	51.31	56.71	46.44	43.68	41.62	46.73	51.39
DIR	67.31	68.52	61.26	60.19	61.11	47.55	65.47	59.82
PR	76.51	69.81	60.04	66.77	61.72	68.62	69.83	59.22
COMB	88.59	87.95	81.24	81.51	80.34	80.07	84.44	78.61

Table 5.17: Subject 1 - Transition time variance(ms) - All Class

Feature	Hammer	3 Jaw Chuck	Ball Squeeze	Door Knob	Key	Scissors	Tip Pinch	Jar Lid
MAG	29	156	53	34	39	63	37	35
XYZ	28	50	54	30	43	45	44	38
MAG 1D	51	322	30	30	48	48	33	29
XYZ 1D	17	121	26	25	27	30	28	25
CANG	39	160	32	75	37	55	43	36
DIR	18	107	39	22	27	31	32	29
PR	29	58	66	37	54	50	44	47
COMB	16	55	29	22	24	35	25	25

Table 5.18: Subject 2 - Transition time variance(ms) - All Class

Feature	Hammer	3 Jaw Chuck	Ball Squeeze	Door Knob	Key	Scissors	Tip Pinch	Jar Lid
MAG	33	121	88	43	40	49	40	49
XYZ	33	95	85	42	46	59	32	51
MAG 1D	148	129	115	25	43	37	38	44
XYZ 1D	22	134	101	22	32	29	41	28
CANG	55	92	120	37	46	74	46	39
DIR	23	116	68	33	28	31	29	27
PR	49	90	87	55	66	60	42	60
COMB	16	83	79	25	25	42	22	34

Table 5.19: Subject 3 - Transition time variance(ms) - All Class

Feature	Hammer	3 Jaw Chuck	Ball Squeeze	Door Knob	Key	Scissors	Tip Pinch	Jar Lid
MAG	37	46	68	29	38	43	52	34
XYZ	33	31	47	34	39	40	39	39
MAG 1D	33	45	57	31	34	42	45	46
XYZ 1D	20	21	35	27	34	32	33	27
CANG	51	49	73	72	82	43	51	78
DIR	18	23	43	28	29	27	39	18
PR	37	42	47	39	46	47	56	49
COMB	26	28	36	35	30	33	34	30

Table 5.20: Subject 4 - Transition time variance(ms) - All Class

Feature	Hammer	3 Jaw Chuck	Ball Squeeze	Door Knob	Key	Scissors	Tip Pinch	Jar Lid
MAG	31	40	38	38	42	66	23	31
XYZ	23	27	40	31	48	41	31	37
MAG 1D	32	22	38	26	33	58	22	35
XYZ 1D	20	20	24	19	20	44	21	31
CANG	36	48	47	45	39	53	52	52
DIR	21	20	29	20	22	44	22	31
PR	37	43	48	43	64	42	53	44
COMB	18	18	27	20	25	29	19	23

Chapter 6: Discussion of Results

For the two class problem the overall classification accuracy averaged for four subjects and all 7 features combined was 86.45%. The transition detection time variance averaged for all subjects, all features combined was 31.12 ms. For the all class problem the overall classification accuracy averaged for four subjects and all 7 features combined was 74.91%. The transition detection time variance averaged for all subjects and all features combined was 30.91 ms.

The results showed that classification accuracy for the two class problem was fairly high when compared to similar research. However, accuracy was about 10% points lower for the all class problem. It is to note that moments of transition were not excluded while measuring classification accuracy. The results also showed that ACC-based features can detect transition very well for both two class and all class problems. When the classifier was trained on individual features, the direction of the axis of rotation of the gravity vector (DIR) was the most effective. It provided two class classification accuracy of approximately 82% and a transition detection time variance of approximately 36ms. However, it was still lower compared to when the classifier was trained on all features combined.

The results are not surprising and can be understood from the time domain plots of the ACC data. Figure 6.1 shows the plot of the magnitude and raw directional data for sensor 8 during one 10 second segment of the hammer grip series. When it comes to certain grip family there is very little difference between characteristics of different phases of prehensile movement. It can be seen that the characteristics of NR and stationary grip phases (HG, HR) are strikingly different from movement phases (HGIN, HGR, HL, HLOUT). However, the characteristics are similar when comparing movement phases to each

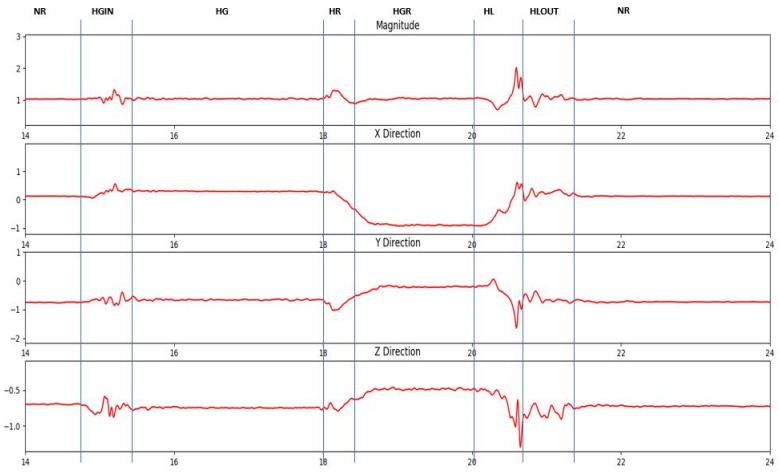

Figure 6.1: A 10 second segment from hammer grip - subject 1

other or stationary phases to each other. Also, from figure 6.2 it can be seen how distinct the DIR feature is around the moments of transition, leading to its superior performance for detecting transitions. When all features are combined they describe motion in more ways than one thus leading to better results when compared to individual features.

The features performed fairly well in detecting transitions. However, it must be considered that the transition detection time variances were averaged due to the 12-fold validation method. If we analyze the boxplot distribution, figure 6.3, it can be seen that there are still some outliers with fairly high transition time variance, up to 800 ms. So the ACC features used do perform well on average in detecting transitions but are slow at certain moments. This is could be explained due to certain moments of transition having significant amount of noise.

Challenges Figure 6.1 shows that certain phases of movement (i.e. HGIN, HR) are very short lasting, occurring for as little as 400 ms. This leads to lower number of samples for the classifier to train on thus leading to lower results for the all class problem. Additionally, certain phases of movement also have very low values, especially around moments of transitions. This magnifies the effect of noise and leads to loss of critical data after filtering.

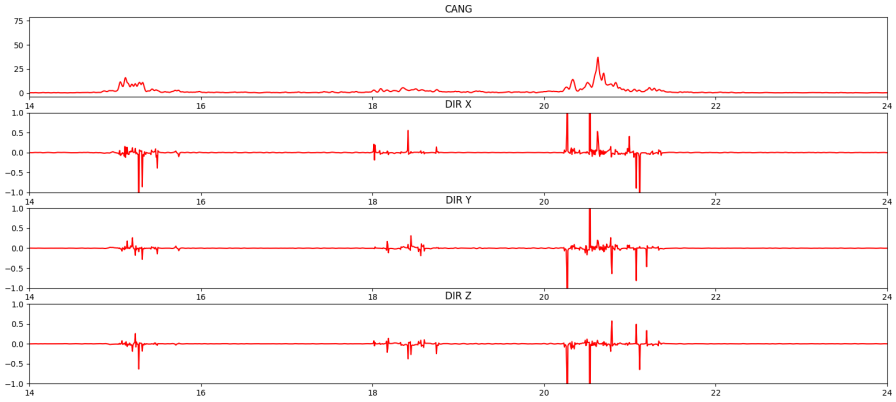

Figure 6.2: CANG and DIR features for hammer grip - subject 1

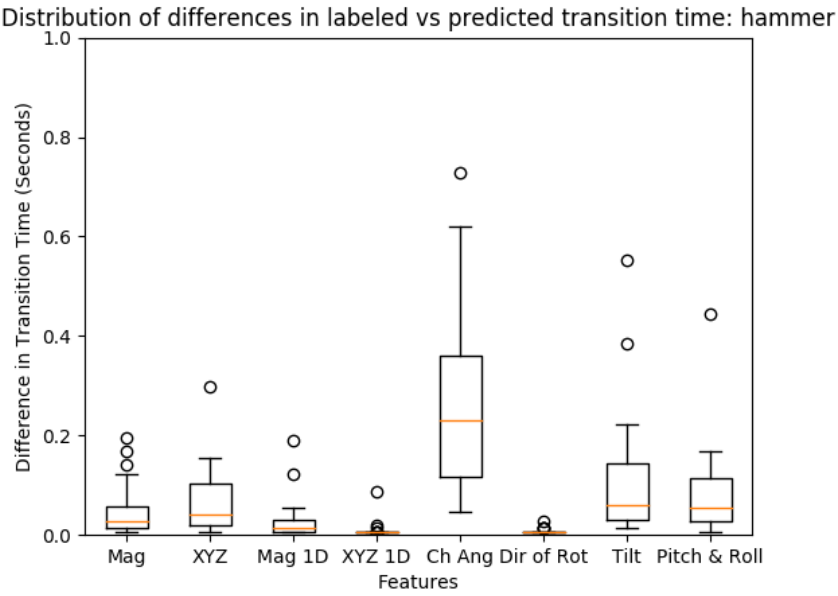

Figure 6.3: Boxplot distribution of transition detection time variance for hammer grip - subject 1

6.1 Conclusion

The ACC-based features used were effective for detecting motion onset and offset, but less effective in detecting all phases of prehensile movement. The direction of the axis of rotation of the gravity vector was very effective in detecting motion onset and offset and movement transitions. This is clinically useful for different use cases that require detecting motion onset and offset. The findings on effectiveness of ACC-based features for recognizing motion transitions may also prove useful for real time control applications. The following objectives were accomplished as part of this research:

- Researched and developed seven features from ACC data.
- Tested the effects of ACC features for classification of prehensile patterns.
- Developed a method to test the performance of classifier for detecting transitions.
- Demonstrated the effectiveness of motion-based features for the two class problem and for detecting transitions.

Chapter 7: Future Work

The following future work is suggested to address the poor performance of ACC features while recognizing all phases of movement.

Hidden Markov Models Random sampling of data was tried for the test and train split. It was scrapped in favor of the current 12-Fold validation method because random sampling caused peaking during the learning process. However, random sampling provided excellent results with both two class and all class classification accuracy in the mid 90s percentile range. This indicates that in order for machine learning to recognize prehensile movement it needs contextual information in the immediate neighborhood of the time instant being tested. Towards that end, Hidden Markov Models (HMMs) could be used since they are most known for recognizing a sequence of activity.

Better Vocabulary for Movement The current descriptions for movements could also be improved or extended. It must be explored whether a movement describing the hammer grip can be simply broken down into just seven labels or does it need more context. Clustering is one technique that could be applied here to determine appropriate enough labeling, classes of movement that could lead to better classification performance. However to truly improve the vocabulary, prehensile movement should be analyzed in a bottom up manner. Each component of prehensile tasks should be analyzed in isolation to see how well it can be recognized using ACC signals. Experiments should be structured requiring the subjects to only perform simple tasks such as moving the index finger instead of complete functional movement such as gripping a hammer. The knowledge learned by analyzing prehensile tasks in isolation can than used to form a vocabulary for movement that is more conducive for machine recognition.

Additional Sensors ACC data used in this thesis came from just three sensors located on the base of the forearm, the little finger, and the thumb. It must be explored whether all eight grip families and all 47 classes of movement, grip and rest used could be recognized with just these three sensors. Further research must be done by using additional sensors perhaps on the biceps of the hand performing prehensile movement.

Bibliography

Bibliography

[1] G. Shuman, Z. Duric, and L. H. Gerber, "Classifying continuous hand grips and movements using myoelectric and accelerometer signals," in *2017 IEEE International Conference on Bioinformatics and Biomedicine (BIBM)*. IEEE, 2017, pp. 608–612.

[2] J. R. Cram, *Cram's introduction to surface electromyography*. Jones & Bartlett Learning, 2010.

[3] L. J. Hargrove, K. Englehart, and B. Hudgins, "A comparison of surface and intramuscular myoelectric signal classification," *IEEE transactions on biomedical engineering*, vol. 54, no. 5, pp. 847–853, 2007.

[4] M. Nordin and V. H. Frankel, *Basic biomechanics of the musculoskeletal system*. Lippincott Williams & Wilkins, 2001.

[5] "Trigno wireless system users guide," https://www.delsys.com/Attachments_pdf/download/users-guides/trigno-wireless-systems.pdf, accessed: 2018-11-22.

[6] A. Keil, T. Elbert, and E. Taub, "Relation of accelerometer and emg recordings for the measurement of upper extremity movement." *Journal of Psychophysiology*, vol. 13, no. 2, p. 77, 1999.

[7] R. M. Murray, *A mathematical introduction to robotic manipulation*. CRC press, 2017.

[8] M. Pedley, "Tilt sensing using a three-axis accelerometer," *Freescale semiconductor application note*, vol. 1, pp. 2012–2013, 2013.

[9] S. J. Russell and P. Norvig, *Artificial intelligence: a modern approach*. Malaysia; Pearson Education Limited,, 2016.

[10] "Electromyography," https://meshb.nlm.nih.gov/record/ui?name=Electromyography, accessed: 2019-02-19.

[11] I. Kuzborskij, A. Gijsberts, and B. Caputo, "On the challenge of classifying 52 hand movements from surface electromyography," in *2012 annual international conference of the IEEE engineering in medicine and biology society*. IEEE, 2012, pp. 4931–4937.

[12] A. Ameri, M. A. Akhaee, E. Scheme, and K. Englehart, "Regression convolutional neural network for improved simultaneous emg control," *Journal of neural engineering*, 2019.

[13] V. Gregori, B. Caputo, and A. Gijsberts, "The difficulty of recognizing grasps from semg during activities of daily living," in *2018 7th IEEE International Conference on Biomedical Robotics and Biomechatronics (Biorob)*. IEEE, 2018, pp. 583–588.

[14] A. Gijsberts and B. Caputo, "Exploiting accelerometers to improve movement classification for prosthetics," in *Rehabilitation Robotics (ICORR), 2013 IEEE International Conference on*. IEEE, 2013, pp. 1–5.

[15] S. A. Moore, A. Hickey, S. Lord, S. Del Din, A. Godfrey, and L. Rochester, "Comprehensive measurement of stroke gait characteristics with a single accelerometer in the laboratory and community: a feasibility, validity and reliability study," *Journal of neuroengineering and rehabilitation*, vol. 14, no. 1, p. 130, 2017.

[16] K. Englehart, B. Hudgins *et al.*, "A robust, real-time control scheme for multifunction myoelectric control," *IEEE transactions on biomedical engineering*, vol. 50, no. 7, pp. 848–854, 2003.

Curriculum Vitae

Nirav Sheth currently works as a information security consultant. He received his Bachelor of Science degree in Computer Science from Southern Polytechnic State University, Marietta GA. He is a member of the International Information System Security Certification Consortium $(ISC)^2$ and a Certified Information Systems Security Professional (CISSP). His research interest include Information Security, Software Development, Machine Learning, and Evolutionary Computation.